Electron scattering from tetrafluoroethylene

R. Panajotovic and M. Jelisavcic
Research School of Physical Sciences and Engineering, Australian National University, Canberra, Australia

R. Kajita, T. Tanaka, and M. Kitajima
Physics Department, Sophia University, Chiyoda-ku, Tokyo, Japan

H. Cho
Physics Department, Chungnam National University, Daejeon 305-764, South Korea

H. Tanaka
Physics Department, Sophia University, Chiyoda-ku, Tokyo, Japan

S. J. Buckman
Research School of Physical Sciences and Engineering, Australian National University, Canberra, Australia

(Received 21 April 2004; accepted 11 June 2004)

We report experimental results for electron scattering from tetrafluoroethylene, C_2F_4, obtained from measurements in two laboratories. An extensive set of differential, integral, and momentum transfer cross sections is provided for elastic scattering for incident electron energies from 1 to 100 eV and inelastic (vibrational excitation) scattering for incident electron energies at 3, 6, 7.5, 8, and 15 eV, and for scattering angles ranging from 10° to 130°. To highlight the role of intermediate negative ions (resonances) in the scattering process we have also measured excitation functions for elastic scattering and vibrational excitation of the ground electronic state of C_2F_4 for incident energies between 1.5 and 20 eV. Our results are compared with recent theoretical calculations and a limited number of other experimental results. © *2004 American Institute of Physics.*
[DOI: 10.1063/1.1778386]

I. INTRODUCTION

Electron collisions with small hydrocarbon molecules like ethylene, for example, and the effect that fluorination has on their electron scattering cross sections, has attracted the attention of both theoreticians and experimentalists for some time.[1–6] There has been considerable spectroscopic research[7–10] and theoretical studies of both ethylene and tetrafluoroethylene up until the 1970s, and the latter molecule has come more into focus recently, due to its important role in low-temperature plasma processing technology. Chemical vapor deposition or etching of doped or undoped silicon-based dielectric layers in the process of semiconductor production is performed with the use of low-temperature plasmas. Fluorocarbons, such as cycloperfluorobutane (c-C_4F_8) and tetrafluoroethylene (C_2F_4) are widely used as precursors for the formation of multilayer connections with low dielectric constants. C_2F_4 is produced either by thermal decomposition of c-C_4F_8, or as a product of the electron or photon interaction with cycloperfluorobutane. Understanding the reaction chemistry of these molecules is crucial for achieving production efficiency and stability of the etched surfaces, but it is equally important when addressing environmental issues since they both present a potential threat to the atmosphere (''green-house'' gases). For example, there is an indication (Olthoff and Christophorou[11]) that the atmospheric lifetime of these pollutants may have been overestimated as low-energy electron-molecule collisions taking place in the upper layers of the Earth's atmosphere have not been considered.

In order to explain the complex collision processes in such low-temperature plasmas, molecular lasers, planetary atmospheres, explosions, etc., a knowledge of absolute differential (DCS), momentum transfer (MTCS), and integral cross sections (ICS) is essential. The formation of molecular negative ion resonances is also particularly interesting in the range of energies spanning from a few hundred meV to a few tens of eV as it is well known that these transient negative ion states can substantially enhance electron scattering cross sections. Their decay can also result in the electron-molecule complex entering channels leading to excitation or fragmentation, producing other active species as a consequence. Being of the same symmetry as $C_2H_4(D_{2h})$, one might expect C_2F_4 to exhibit similar resonant behavior at energies below 10 eV. Therefore, there is a special interest in a detailed analysis of excitation functions (EF) for elastic scattering and vibrational excitation in this energy range.

There have been just a few experimental[1,2,6] and theoretical[3–5] studies regarding electron impact cross sections of tetrafluoroethylene. Coggiola *et al.*[1] reported the only experimental results where DCS were measured for elastic and inelastic electron scattering using a standard crossed-beam technique. Their measurements were relative and were normalized to an arbitrary value of 1×10^{-16} cm^2/s, at both of their incident energies (25 and 40 eV) at a scattering angle of 40°. Also, their experiment was limited to measurements at angles from 0° to 80°. They examined the effect that a substitution of one or more of the hydrogen atoms in ethylene by fluorine atoms has on the electron scattering interaction. In previous optical studies, Bélanger and Sandorfy[10] revealed that all molecules in the series

(C_2H_4,C_2H_3F,…,C_2F_4) have a strong $\pi(^1b_{3u})\rightarrow\pi^*(^1b_{2g})$ (highest occupied→lowest unoccupied molecular orbital) transition, but that only tetrafluoroethylene has a large blue shift of 1.2 eV. From the two states produced in the $\pi\rightarrow\pi^*$ transition, $1\,^3B_{1u}$ and $1\,^1B_{1u}$, only the singlet state has a large optical oscillator strength and consequently was visible in the optical spectrum taken in the range from 200 to 115 nm (6.2 to 10.8 eV).

In their electron scattering experiment Coggiola *et al.* looked not only at the singlet but also at the triplet state, $1\,^3B_{1u}$, and observed a peak in the energy-loss spectrum at 4.68 eV, just slightly shifted compared to other molecules in the series. This suggested that a significant change of configuration is taking place in tetrafluoroethylene, which is different to that observed in the other fluorinated hydrocarbons. This was discussed in detail by Chiu, Burrow, and Jordan[2] who performed an electron transmission experiment on the same group of molecules. They focused on investigating temporary negative molecular ions (molecular resonances) and found that increased fluorination is effectively destabilizing the π^* negative ion orbital. Their explanation was based on the assumption that the considerable shortening of the C—C bond stabilizes the bonding orbital and destabilizes the antibonding, while the same effect in the C—F bond destabilizes both π and π^*. This has led to a conclusion that the π orbital is almost unchanged while π^* is considerably destabilized compared to that in ethylene. As a consequence, the ionization potential of the π orbital in C_2F_4 is almost the same as in ethylene, but the electron affinity is much higher. This is in accordance with their observation for the energy of the π^* resonance at 1.8 eV in ethylene, whilst it is found at 3 eV in C_2F_4.[2] The other investigation where cross sections and resonances have been studied is the combined analysis of electron transport data and *ab initio* theoretical calculations by Yoshida *et al.*[12] They computed elastic momentum transfer cross sections as well as cross sections for electronic excitation and used these, together with model vibrational excitation cross sections, to obtain an optimum cross section set by fitting to the transport data using a Boltzmann equation approach. The theoretical cross sections used in this set were calculated using the Schwinger variational technique and the method used has been reported separately.[4] Up until the present, the set of cross sections for electron impact on C_2F_4 provided by Yoshida *et al.*[12] was the main source of information for researchers investigating the chemistry of C_2F_4 plasma discharges. Recently there has been another set of calculations for elastic scattering from C_2F_4 by Trevisan, Orel, and Rescigno,[5] who used the complex Kohn variational technique. In a following section we will compare the results of both of these theoretical approaches to the present cross section data, and indicate where there are some significant differences as well as some significant successes.

At the grand total cross section level there is a theoretical calculation from 30 to 3000 eV by Jiang, Sun, and Wan[3] for which they applied an energy-dependent, geometric additivity rule approach, and recent experimental results using the electron-transmission technique by Szmytkowski, Kwitnewski, and Ptasinska-Denga[6] for energies from 0.6 to 370 eV. These are a very useful reference for the magnitude of the overall electron-C_2F_4 scattering process.

The theoretical analysis of Winstead and McKoy,[4] mentioned above, applied the static-exchange approximation. Polarization effects were considered only in the calculation of the *total* elastic cross section and only for the $^2B_{1u}$, $^2B_{2g}$, and $^2B_{2u}$ symmetries. They were not included in the calculation of the differential elastic or elastic or momentum transfer cross sections. They obtained, using the Schwinger multichannel method, positions for several molecular resonances in both elastic and electronic excitation cross sections. The Kohn calculations of Trevisan, Orel, and Rescigno[5] produced elastic scattering differential cross sections for energies between 0.5 and 20 eV. They used effective core potentials in their description of the target and a mix of static-exchange (SE) and polarized self-consistent field (SCF) wave functions to treat the various scattering symmetries. The SE approximation was used for the $^2B_{1g}$ symmetry, the polarized SCF approach for the ^2A_g, $^2B_{3g}$, and $^2B_{3u}$ symmetries, and what they refer to as the ''relaxed SCF'' approach for the $^2B_{1u}$, $^2B_{2g}$, and $^2B_{2u}$ symmetries. They also found a number of resonances in the various scattering symmetries and these results will be compared with the present experiment and discussed in a later section.

The main objective of our experimental studies was to provide a complete set of differential, integral, and momentum transfer cross sections for elastic electron scattering and the vibrational excitation of the ground electronic state of tetrafluoroethylene. We have measured absolute elastic differential cross sections for electron scattering from C_2F_4 at a number of energies between 1.5 and 100 eV and at scattering angles from 20° to 130°. We also calculated ICS and MTCS by extrapolating the DCS to 0° and 180° and integrating the resultant cross section. This was assisted by the use of a molecular phase shift analysis technique, applied previously to our measurements on ethylene (Panajotovic *et al.*[13]), which removes some of the subjectivity from the extrapolation process.

II. EXPERIMENTAL APPARATUS AND TECHNIQUES

This work was carried out as a collaboration between three laboratories, with the experimental work being performed in two of them—the Australian National University (ANU) and Sophia University (SU). A detailed description of the apparatus used in both laboratories has been given in a previous publication,[14] so we will only briefly discuss the relevant aspects here.

Both the ANU and SU measurements are performed on traditional crossed-beam spectrometers consisting of an electron monochromator and an analyzer, which collects electrons, scattered at different angles after the collision with the molecular target. In both, the energy selectors are hemispherical electrostatic elements. The overall energy resolution of the spectrometer was ~50 meV at ANU and 25–30 meV at SU. The absolute value of the incident energy was determined through calibration against the well-known positions of the quasivibrational structures of the N_2 negative ion (low energies),[15] or against the $1s2s^2\,^2S$ resonance in He for energies above 10 eV.[16] In order to put measured scattering

intensities on an absolute scale, we used the relative flow technique, described also in detail elsewhere.[14] The basic requirement of this method is that identical scattering conditions are provided for both the target and the standard gas (helium), so that the scattering signal from the target can be compared with that of the standard gas for which there is an accurate set of differential cross sections established by Nesbet,[17] Boesten and Tanaka,[18] and theoretical close-coupling calculations (Fursa and Bray[19]). There are slight differences in the operation of the experiment at ANU and Sophia. At the ANU the target beam was flowing through a 1 mm wide and 18 mm long capillary tube, while at Sophia the capillary was thinner and shorter. Typical driving pressures used at ANU were 0.15 Torr (C_2F_4) and 1 Torr (He) while at SU the pressures were in the same proportion but approximately five times higher. The mean free path for tetrafluoroethylene was assumed to be similar to that of ethylene,[13] as there is no reliable data for the hard-sphere diameter of C_2F_4 available in the literature. While this imposes some uncertainty on the correct pressure ratio for use in the experiments, measurements of the elastic cross section as a function of this ratio in a small range about the calculated value (C_2F_4/He ~ 6) indicate that this is not a significant issue.

Both spectrometers can be operated in two modes: in one, the angular dependence of the scattered signal is measured at a fixed impact energy and energy loss, while in the other, energy loss and scattering angle are fixed and the incident energy is varied. In the first mode absolute angular DCS are obtained while in the second, absolute excitation functions for either elastic scattering or vibrational excitation are measured. The absolute uncertainties varied with both angle and scattering process but they were generally below $\sim$15% for elastic scattering and $\sim$20% for vibrational excitation. The corresponding integral and momentum transfer cross sections have estimated uncertainties of $\sim$25%.

III. RESULTS AND DISCUSSION

A. Elastic scattering

Absolute differential cross sections for elastic electron scattering from C_2F_4 are presented in Table I, while in Figs. 1 and 2 we make comparisons between the present results and the theoretical calculations, as well as with the measurements of Coggiola *et al.*[1] at one of the two energies where that is possible. In general the level of agreement between the ANU and SU cross sections is very good at all energies where they overlap. There are some differences, however, and these are discussed below.

In Figs. 1(a)–1(d) we see that the angular dependence of the cross section changes quite rapidly for energies between 1.5 and 5 eV. At low energies there is a shallow minimum at about 40° and the DCS is almost flat at larger angles. However, by 5 eV this forward-angle minimum has disappeared to reveal a DCS which is forward peaked and has a minimum developing at about 100°. Between 5 and 20 eV [Figs. 2(a)–2(d)], the DCS does not change much in shape, but its magnitude at forward angles grows considerably. The only other experimental measurements with which comparison can be made are those of Coggiola *et al.* This has been done by normalizing their 25 eV data to the ANU cross section at an incident electron energy of 20 eV and at a scattering angle of 60°. The result is shown in Fig. 2(d) and the agreement with both the ANU and SU data is excellent.

We also compare, throughout Figs. 1 and 2, with calculated cross sections from both of the theoretical approaches, and the result is quite mixed. At energies below about 5 eV, the level of discrepancy between the experiments and both calculations is significant. This is particularly true for the Schwinger calculation which, for example, overestimates the DCS by about an order of magnitude at forward angles and an energy of 1.5 eV. As the energy increases (e.g., 2 and 3 eV) there is improved agreement between experiment and theory, particularly at backward angles and particularly with the Kohn calculation. At 5 eV the agreement in magnitude with the Kohn calculation is good, although there are some differences in the shape of the DCS at midangles. The Schwinger calculation is still larger in magnitude than the experiment but the agreement is significantly better than at lower energies. At energies above 10 eV the agreement between experiment and theory is generally very good.

The disagreement between experiment and theory for the elastic DCS at low energies and small scattering angles seems to be a long-standing problem, not only with this molecule, but also with low-energy (<5 eV) electron scattering measurements from many other molecules (C_2H_4,[13] N_2O,[14] SF_6,[20] diatomic molecules[21]). Reproducing the detailed behavior of the elastic DCS in this regime obviously provides a critical test of scattering calculations.

It is also apparent from Figs. 1 and 2 that there are some significant differences (outside combined error bars) between the present measurements from our two laboratories, particularly at low energies (e.g., 3 and 5 eV) and small scattering angles, and at 8 eV and larger scattering angles. While the source of these discrepancies is not presently understood, they are the exception rather than the norm and do not have a significant bearing on the conclusions that we draw here, particularly with regard to the comparison with theory.

The discrepancies that are evident between experiment and theory for the DCS are also reflected in the comparison of the calculated ICS and MTCS and the values derived from the present DCS measurements, which are presented in Figs. 3(a) and 3(b), respectively. Both the present results and the recent total cross section measurements of Szmytkowski, Kwitnewski, and Ptasinska-Denga[6] indicate that the elastic integral cross section of Winstead and McKoy is too high at energies below 10 eV. On the other hand, the calculation of Trevisan, Orel, and Rescigno provides an excellent overall description of the ICS. The measured momentum transfer cross sections [Fig. 3(b)] agree relatively well with both calculations between 5 and 20 eV, reflecting the better level of agreement between experiment and theory at the DCS level at backward angles in this energy range. However, once again the Schwinger calculation cross section greatly overestimates the cross section at low and high energies, while the Kohn technique provides a reasonable description of the cross section magnitude at all energies.

The calculated integral cross sections for elastic electron scattering (Winstead and McKoy,[4] Trevisan, Orel, and

TABLE I. Differential cross sections for elastic electron scattering from tetrafluoroethylene, in units of 10^{-16} cm^2/sr. The ANU measurements are labeled (*A*) and the Sophia measurements (*S*). The absolute uncertainty for ANU measurements is given in parentheses (%) and for the Sophia measurements it is ±15%. Integral and momentum transfer cross section are given in units of 10^{-16} cm^2 and the uncertainty is estimated to be between 20% and 25%.

	Energy (eV)						
Angle	1.5 (*A*)	1.5 (*S*)	2 (*S*)	3 (*A*)	3 (*S*)	4 (*S*)	5 (*A*)
20		0.596	0.539	1.88(50)	0.781	0.842	2.66(7)
30	0.649(12)	0.399	0.356	0.993(7)	0.627	0.950	2.00(12)
40	0.352(12)	0.250	0.287	0.756(7)	0.701	0.969	1.90(12)
50	0.257(19)	0.247	0.346	0.816(10)	0.802	1.091	1.51(7)
60	0.331(8)	0.330	0.392	0.681(7)	0.756	0.954	1.14(8)
70	0.363(9)	0.352	0.417	0.578(7)	0.719	0.755	0.834(7)
80	0.390(8)	0.393	0.435	0.487(7)	0.589	0.537	0.629(6)
90	0.380(8)	0.412	0.367	0.426(6)	0.563	0.480	0.507(7)
100	0.394(10)	0.433	0.343	0.377(8)	0.501	0.409	0.441(7)
110	0.368(9)	0.410	0.320	0.364(9)	0.440	0.385	0.394(9)
120	0.360(9)	0.413	0.306	0.360(7)	0.402	0.348	0.392(7)
130	0.363(9)	0.366	0.286	0.364(7)	0.410	0.349	0.428(7)
ICS	4.86	4.55	4.34	7.37	7.13	7.73	10.9
MTCS	3.89	4.13	3.70	5.06	5.84	5.90	6.78

	Energy (eV)						
Angle	5 (*S*)	6 (*S*)	7 (*S*)	7.5 (*A*)	8 (*S*)	9 (*S*)	10 (*A*)
20	1.487	2.455	2.388	3.39(7)	3.149	3.427	5.09(7)
30	1.587	2.477	2.301	2.67(7)	2.698	2.981	3.46(7)
40	1.621	2.263	1.965	2.17(7)	2.058	2.168	2.54(7)
50	1.555	1.880	1.521	1.50(7)	1.572	1.600	1.64(6)
60	1.211	1.323	1.083	1.06(7)	1.048	1.166	1.19(7)
70	0.911	0.928	0.873	0.814(6)	0.966	1.049	1.03(6)
80	0.652	0.725	0.760	0.741(7)	0.867	0.922	0.943(7)
90	0.579	0.672	0.683	0.670(6)	0.882	1.014	0.864(7)
100	0.529	0.580	0.607	0.607(7)	0.809	0.913	0.793(6)
110	0.479	0.528	0.594	0.586(7)	0.788	0.840	0.793(6)
120	0.427	0.531	0.661	0.632(6)	0.845	0.935	0.865(5)
130	0.511	0.621	0.803	0.786(7)	0.955	1.104	1.02(6)
ICS	10.1	13.1	10.5	13.4	14.4	16.8	19.8
MTCS	7.38	8.37	7.62	9.24	11.6	12.5	15.1

	Energy (eV)							
Angle	10 (*S*)	15 (*A*)	15 (*S*)	20 (*A*)	20 (*S*)	30 (*S*)	60 (*S*)	100 (*S*)
20	4.594	8.37(8)	7.896	9.10(7)	8.781	9.537	6.75	2.80
30	3.312	4.77(8)	4.233	3.74(6)	3.866	2.970	1.44	1.29
40	2.428	2.32(8)	2.373	1.80(6)	1.815	1.298	0.940	0.645
50	1.605	1.43(8)	1.365	1.15(7)	1.173	1.064	0.642	0.332
60	1.222	1.07(7)	1.085	1.04(7)	1.101	0.911	0.437	0.229
70	1.022	0.922(7)	0.981	0.881(7)	0.934	0.753	0.245	0.185
80	0.979	0.827(10)	0.830	0.725(8)	0.861	0.543	0.202	0.157
90	0.896	0.696(6)	0.808	0.585(7)	0.660	0.387	0.177	0.114
100	0.869	0.650(8)	0.711	0.529(8)	0.540	0.332	0.172	0.106
110	0.852	0.629(8)	0.711	0.575(6)	0.578	0.446	0.221	0.140
120	0.896	0.760(11)	0.771	0.769(9)	0.795	0.558	0.328	0.205
130	1.053	0.969(8)	0.983	1.08(7)	1.034	0.773	0.441	0.288
ICS	19.4	19.0	18.7	22.2	20.8	16.9	12.2	5.43
MTCS	15.8	11.0	12.7	15.8	16.1	9.64	4.66	2.72

Rescigno[5]) reveal several resonance structures: a sharp resonance of $^2B_{2g}$ symmetry is seen in both calculations although at slightly different energies (3.6 and 3.1 eV, respectively), one at around 4.6 eV of $^2B_{2u}$ symmetry, two at 7.3 and 19.4 eV of the $^2B_{1u}$ symmetry, and broad resonances of ^2A_g and $^2B_{3g}$ symmetry at 12.5 and 20 eV, respectively. Of all these predicted resonances, only the ~3 eV resonance has been confirmed to date in the experiment of Chiu Burrow, and Jordan.[2] It corresponds to the well-known π^* shape resonance found in ethylene at 1.8 eV. As discussed by Winstead and McKoy (and references therein) the difference in the energy of this resonance in C_2F_4 may be due to the nonplanar structure of the $C_2F_4^-$ ion—a lowest-energy orientation (chair) structure of C_{2h} symmetry, with pairs of fluorine atoms attached to carbon atoms being bent upwards and downwards with respect to the C═C bond plane. A normal mode

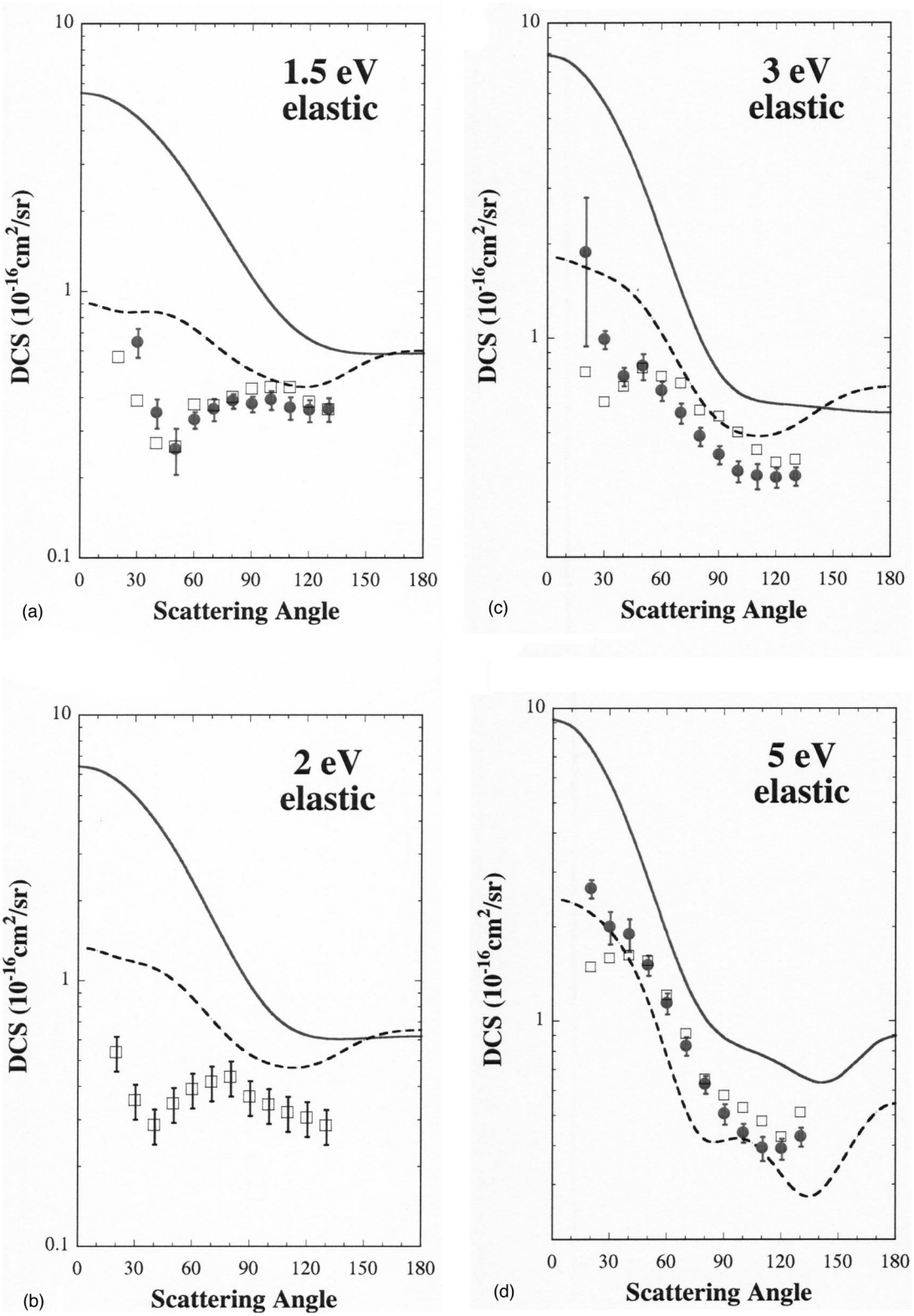

FIG. 1. Absolute differential cross sections (10^{-16} cm^2 sr^{-1}) for elastic scattering from C_2F_4 at (a) 1.5 eV, (b) 2 eV, (c) 3 eV, and (d) 5 eV. Present results are shown as (●) ANU and (□) Sophia. The (——) Schwinger variational calculation (Ref. 4) and (— — —) Kohn variational calculation (Ref. 5) are also shown.

of C_2F_4 that corresponds to this deformation is therefore expected to be preferentially excited. The difference between the experimental and calculated position of the resonance is probably due to an inadequate representation of polarization effects in the theoretical model, as suggested by Winstead and McKoy. This is supported by the better agreement, with regard to position, found between experimental results and the Kohn variational calculation.

In order to make a closer investigation of the resonances predicted by theory in the energy range from 1.5 to 20 eV,

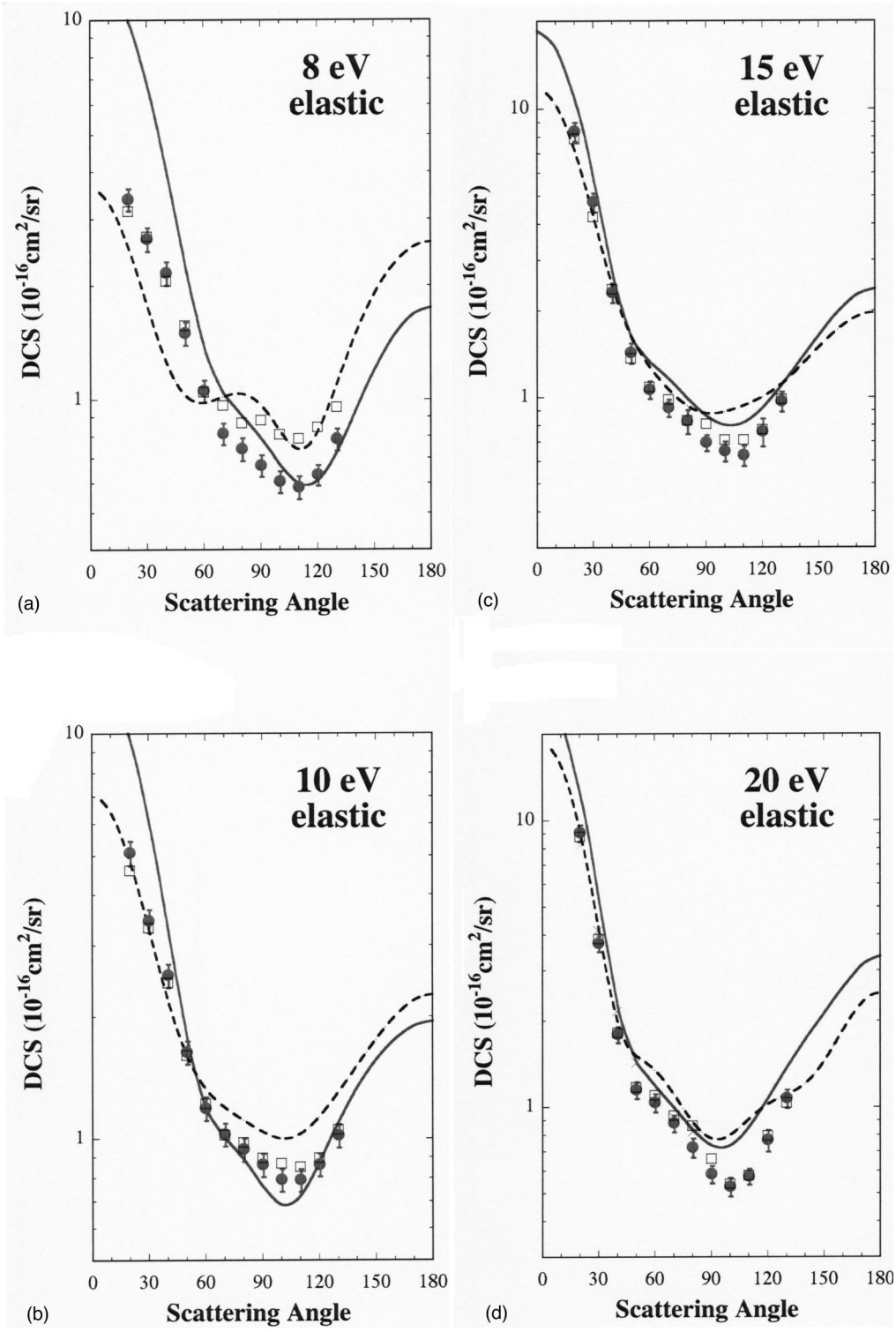

FIG. 2. Absolute differential cross sections (10^{-16} cm^2 sr^{-1}) for elastic scattering from C_2F_4 at (a) 8 eV, (b) 10 eV, (c) 15 eV, and (d) 20 eV. Present results are shown as (●) ANU and (□) Sophia. The measurements of (×) Coggiolla *et al.* (Ref. 1) and the (——) Schwinger variational calculation (Ref. 4) and (— — —) Kohn variational calculation (Ref. 5) are also shown.

we measured the energy dependence (excitation functions, or EF) of the elastic cross section at three scattering angles 60°, 90°, and 120°, and these are shown in Fig. 4, together with the ANU and SU DCS data at several fixed incident energies. The agreement between the EF data and DCS data is within error bars, as well as the agreement between the ANU and SU DCS data (as has been shown in Figs. 1 and 2). The excitation functions are relatively featureless but indicate weak features at ~3.5, 5, and 10–14 eV. These may well be associated with the $^2B_{2u}$ (window-and-peak) and $^2B_{1u}$ (pure "window") resonances.[4] Interestingly, there is little sign of the π^* structure at 3 eV in these elastic excitation functions, which suggests that the $^2B_{2g}$ resonance does not influence the elastic cross section at all. This is in contrast to the situ-

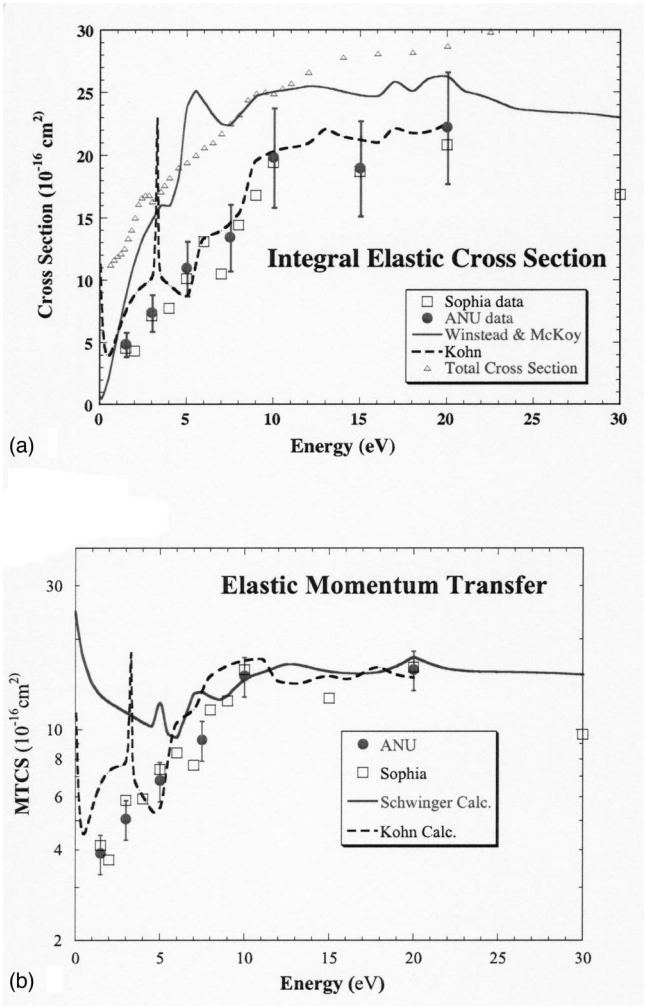

FIG. 3. (a) Integral elastic and (b) elastic momentum transfer cross sections (10^{-16} cm^2) for C_2F_4. Present results are shown as (●) ANU and (□) Sophia. The (——) Schwinger variational calculation (Ref. 4) and (— — —) Kohn variational calculation (Ref. 5) are also shown as is the total cross section of Szmytkowski, Kwitnewski, and Ptasinska-Denga (Ref. 6).

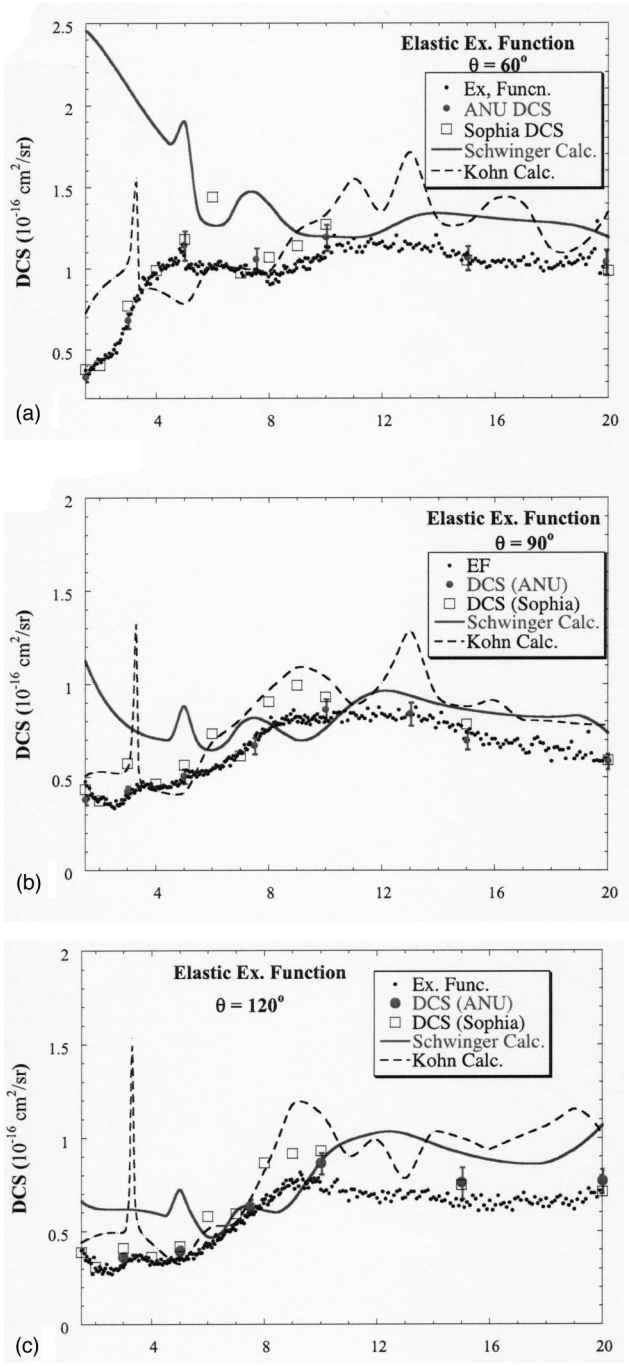

FIG. 4. The energy dependence (excitation function) of the elastic scattering cross section measured at (a) 60°, (b) 90°, and (c) 120°. The small solid points represent the excitation function while the present angular DCS results are shown as (●) ANU and (□) Sophia. The (——) Schwinger variational calculation (Ref. 4) and (— — —) Kohn variational calculation (Ref. 5) are also shown.

ation in C_2H_4 where the resonance has been shown to strongly influence the elastic cross section (Panajotovic *et al.*[13]). The origin of a broad structure between 10 and 14 eV, seen in both the 60° and 90° spectra, is unknown, but it may be associated with one or more of the higher energy resonances predicted in both calculations.

B. Vibrational excitation

Tetrafluoroethylene has 12 fundamental vibrational modes. The symmetry of the vibrational states of the ground electronic state, the type of deformation associated with certain modes, and the frequencies of these modes are listed in Table II.[7–9] It is clear that many of these modes overlap and that they could not be resolved with either of our spectrometers. An example of what has been observed with the higher resolution Sophia spectrometer is presented in Fig. 5 where we show an energy-loss spectrum for an incident electron energy of 3 eV, corresponding to the energy of the π^* resonance. This shows that those fundamental modes with an excitation energy of less than ~50 meV cannot be resolved from the elastic peak and that the rest of the modes, and possible overtones, produce two broad peaks at ~120 and 230 meV. Although we do not show it explicitly, it is interesting to note that the peak in the 3 eV spectrum at ~120 meV apparently ''shifts'' to a higher energy loss, in similar energy-loss spectra recorded at 7.5 eV with both spectrometers. In the latter case the lowest energy-loss peak occurs at ~160 meV and most likely corresponds to excitation of the ν_5 and ν_{10} vibrational modes.

TABLE II. Fundamental vibrational modes of tetrafluoroethylene (from Ref. 7).

Symmetry		Type of deformation	Energy (meV)	Type
A_u	ν_4	CF_2 twist	23.6	Infrared-combination
B_{2u}	ν_{10}	CF stretching	27.0	Infrared
A_g	ν_3	CF_2 scissor	48.9	Raman
B_{1u}	ν_7	CF_2 wag	50.6	Infrared-combination
B_{2g}	ν_8	CF_2 wag	63.0	Raman
B_{1g}	ν_6	CF_2 rock	67.6	Infrared-combination
B_{3u}	ν_{12}	CF_2 scissor	69.2	Infrared
A_g	ν_2	CF stretching	96.64	Raman
B_{3u}	ν_{11}	CF stretching	147.3	Infrared
B_{2u}	ν_9	CF_2 rocking	165.7	Infrared-combination
B_{1g}	ν_5	CF_2 stretch	166.5	Raman
A_g	ν_1	C═C stretching	232.6	Raman

As can be seen from Table II there are no fundamental vibrations at this lower energy-loss value (120 meV) and we suspect that this peak is a combination of overtones, possibly of the ''rocking'' and ''wagging'' (Table II) vibrations. For instance one possibility is that at 3 eV the resonance decay may lead to excitations such as $2\nu_8$, which would result in a feature at 126 meV. We also cannot rule out the possibility that this peak may be due to scattering from vibrationally excited molecules that are thermally excited in the molecular beam. For example, the energy loss of 0.12 eV matches closely the transition from ν_4 to ν_{11} or ν_{10} to ν_{11} within the present resolution. Initial Maxwell-Boltzmann populations for vibrationally excited states of C_2F_4 at 323 K are shown in Table III and one can see that a relatively large population of the ν_4 and ν_{10} states is expected, and this could contribute to the present energy-loss spectra shown in Fig. 5. Off-plane nuclear motion of the ν_4 excitation may lead to a resonant enhancement of the $\nu_4 \rightarrow \nu_{11}$ excitation via the nonplanar structure of the $^2B_{2g}$ shape resonance at around 3 eV.

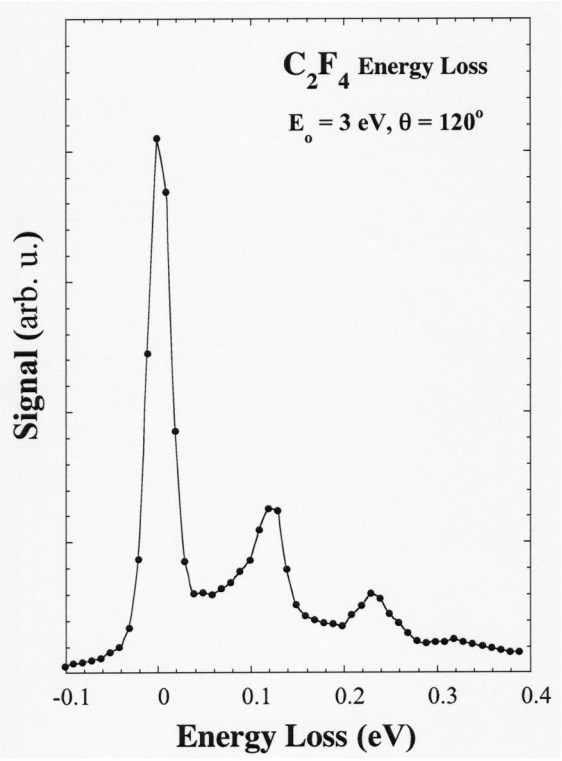

FIG. 5. The energy-loss spectrum for C_2F_4 at an incident energy of 3 eV and a scattering angle of 120°.

TABLE III. Initial population for vibrational excited states of C_2F_4 at 323 K.

C_2F_4		
State	Energy (meV)	Population
Ground state	0	1
ν_4	23.6	0.392
ν_{10}	27.0	0.335
ν_3	48.9	0.172
ν_7	50.6	0.162
$2\nu_4$	47.2	0.153
$\nu_4+\nu_{10}$	50.6	0.131
$2\nu_{10}$	54.0	0.112
ν_8	63.0	0.102

Finally, we note that the energy-loss peak at 0.12 eV is seen in both experiments but is significantly more prominent in the SU spectra and may be due to the fact that the beam temperature in the SU apparatus is ~50 °C, while in the ANU spectrometer it is ~22 °C. However, this possibility does not explain why the 0.12 eV peak is only observed in the energy region of the π^* resonance. Its appearance may therefore be due to a combination of effects involving both vibrationally excited target molecules and/or a preference for the decay of the resonance to a combination mode of vibrationally excited states.

Differential cross sections for vibrational excitation of C_2F_4 are given in Table IV and shown in Fig. 6. The absolute uncertainties are higher than in the case of the elastic DCS, mainly due to lower statistical accuracy. For an incident elec-

TABLE IV. Differential cross section (DCS) for vibrational excitation of tetrafluoroethylene, in units of 10^{-16} cm^2/sr. Note that the energy loss is 0.12 eV for an energy of 3 eV, and 0.16 eV for all other energies. The ANU measurements are labeled (*A*) and Sophia University measurements (*S*). The absolute uncertainty for the ANU measurements is given in parenthesis (%) and for Sophia measurements it is ±15%.

	Energy (eV)					
Angle (deg)	3 (*A*)	3 (*S*)	6 (*S*)	7.5 (*A*)	8 (*S*)	15 (*A*)
20	0.248(32)	0.044		0.163(19)		0.053(46)
30	0.187(26)	0.040	0.085	0.094(20)	0.089	0.048(26)
40	0.081(21)	0.047		0.062(17)		0.033(31)
50	0.154(43)	0.060		0.074(13)		0.018(21)
60	0.095(13)	0.061	0.073	0.074(13)	0.070	0.016(20)
70	0.098(13)	0.074		0.069(13)		0.016(16)
80	0.102(12)	0.083		0.068(12)		0.017(18)
90	0.107(13)	0.098	0.088	0.063(13)	0.056	0.019(22)
100	0.111(13)	0.104		0.060(13)		0.020(22)
110	0.121(13)	0.111		0.061(12)		0.019(25)
120	0.125(12)	0.125	0.064	0.062(13)	0.054	0.019(19)
130	0.128(12)	0.148		0.062(13)		0.018(27)

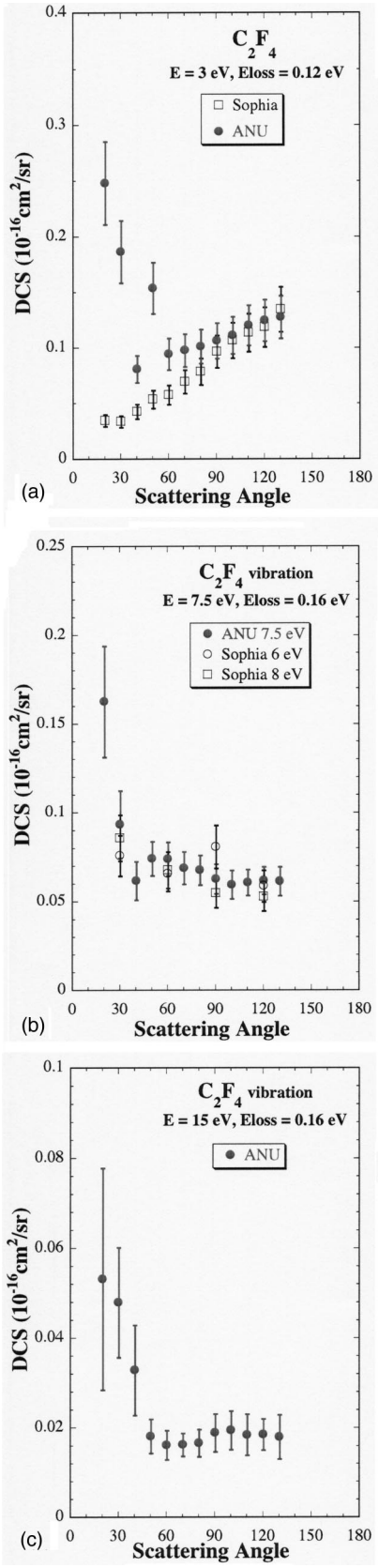

FIG. 6. Absolute differential cross sections (10^{-16} cm^2 sr^{-1}) for vibrational excitation of C_2F_4 (a) at an incident energy of 3 eV and energy loss of 0.12 eV; (b) at an incident energy around 7 eV and energy loss of 0.16 eV; (c) at an incident energy of 15 eV and energy loss of 0.16 eV. Both (●) ANU and (□), (○) Sophia data are shown.

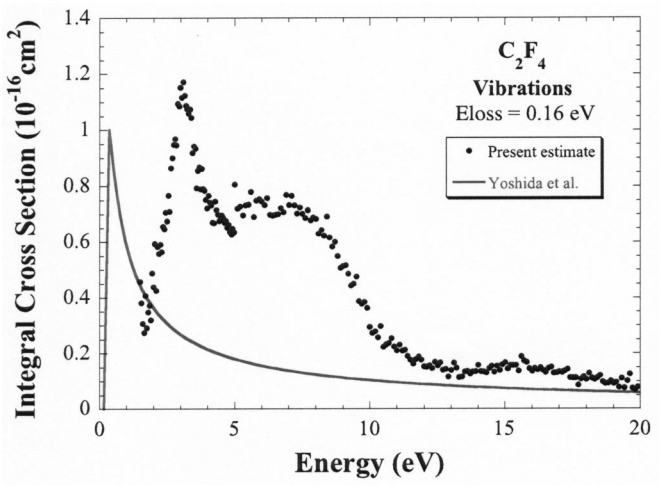

FIG. 7. Integral cross section (10^{-16} cm^2) for vibrational excitation of C_2F_4 at an energy loss of 0.16 eV. The present results (●) are compared with the cross section of Yoshida *et al.*[12]

tron energy of 3 eV, both the ANU and the SU DCS are measured for an energy loss of 120 meV. As these measurements involve determining the ratio of vibrational to elastic scattering in order to obtain the absolute scattering cross section, a large part of this difference results from the differences observed in the elastic scattering measurements at this energy and these angles. Another possible explanation for this discrepancy could be the different initial vibrational populations in the target beams, as we have already mentioned. For incident energies of 7.5 and 15 eV, and for an energy loss of 0.16 eV, the DCS has been measured at ANU, while at energies of 6 and 8 eV, measurements have been performed at SU at four scattering angles (30°, 60°, 90°, and 120°). By deconvoluting the higher resolution SU spectra it was found that the largest contribution to the 0.16 eV energy-loss peak comes from the excitation of the ν_5, ν_{10}, and ν_{11} modes (Table II). The most dominant contribution is most likely coming from the $\nu_5\,(B_{1g})$ and $\nu_{10}\,(B_{2u})$ "stretching" modes since they are strongly (Raman and infrared, respectively) active in the optical spectrum. Due to the small energy difference between these modes, we were not able to resolve them in the experiment. Therefore, the cross sections at 6 and 8 eV, in Table IV and Fig. 6, represent the sum of all three vibrational excitations. Comparison between the 6, 7.5, and 8 eV DCS shows very little difference between them, which is not surprising, given the broad width of the resonance at this energy (see, for example, Fig. 7). Also, the DCS is larger at lower energies, being almost an order of magnitude larger at 3 eV than at 15 eV, and while it is smaller in magnitude at 6, 7.5, and 8 eV, it is still considerably larger than at 15 eV. This, amongst other possible mechanisms, is clearly a consequence of the resonant enhancement of the scattering cross section at 3 eV and ~7.5 eV.

We assume that the $A_g\,(\nu_1)$ mode—stretching of the C═C double bond—is dominant in the second broad peak at 230 meV energy loss. However, no further measurements have been done at this energy-loss value due to the low signal intensity.

In order to make a comparison with the integral vibra-

tional excitation cross sections derived by Yoshida *et al.*[12] from their electron swarm analysis, we have used our absolute vibrational EFs and absolute vibrational DCS measurements to estimate an integral vibrational cross section for an energy-loss value of 0.16 eV. This ICS was obtained by simply averaging the measured EFs at 60°, 90°, and 120°, and then scaling the resultant average by 4π–based on the observation that the EFs differed very little across this angular range and the measured vibrational DCS (see Fig. 6) show only weak angular dependence. We stress that this is only an estimated vibrational ICS, but it does enable us to make some interesting comparisons with the recommended cross section of Yoshida *et al.* In Fig. 7 we show the present vibrational ICS together with that from the Yoshida *et al.* model. The present integral cross section clearly shows strong resonant enhancement at 3 eV where a broad (~1.5 eV wide) and prominent peak (the π^* resonance) dominates the cross section. Note that this resonance does not manifest strongly in the elastic excitation function. Another, broader resonance follows in the region from 6 to 9 eV and then, a much smaller and very broad resonance is observed between 13 and 18 eV. As we have already mentioned, this is very much in contrast to ethylene (Panajotovic *et al.*[13]), where the π^* resonance contributes significantly to both the elastic and vibrational excitation cross sections. It is also clear that a comparison with the ICS of Yoshida *et al.* reveals significant differences. As we have discussed previously, the Yoshida *et al.* cross section is obtained from an analysis of electron swarm measurements. This is achieved by postulating a set of cross sections and manipulating their energy dependencies and magnitudes in such a way that transport coefficients, obtained from solving the Boltzmann equation with this cross section set, match values measured in the experiment. To estimate the contribution from vibrational excitation in their model, Yoshida *et al.* considered cross sections for two vibrational ''modes,'' at 0.16 and 0.23 eV, and assumed that the energy dependence of the cross sections could be approximated by using the Born-dipole approach, with a cross section maxima at ~1 eV in each case. This cross section form is then scaled to give best agreement with the transport data, and the scaling factor, which should be applied to their cross section as shown in Fig. 7 is 11.7. The most striking difference between the model cross section and the measured ICS is the shape. It is also apparent that, after scaling, the model cross section probably significantly overestimates the extent of vibrational excitation and clearly provides the wrong energy dependence. It would be interesting to see the effect that the use of the present cross sections have on the swarm analysis for C_2F_4 or indeed in the modeling of C_2F_4; and C_4F_8 gas discharges.

IV. CONCLUSIONS

In order to provide a complete set of electron scattering cross sections for C_2F_4, and a deeper insight into the dynamics and coupling between negative ion resonances and the ground and vibrational modes of the neutral tetrafluoroethylene molecule, we have measured absolute differential cross sections for elastic scattering at energies spanning from 1.5 to 100 eV and excitation functions from 1.5 to 20 eV incident electron energies. At energies above 5 eV the measured cross sections are well reproduced by theory, both the Schwinger variational approach and the complex Kohn technique. At energies below 5 eV, there are discrepancies between experiment and both theoretical approaches, the most significant being the Schwinger calculation. This is no doubt due to the lack of inclusion of polarization effects in this calculation.

For vibrational excitation, we have measured both absolute excitation functions and absolute DCS at three energies where the excitation functions clearly indicate the presence of resonances. We have shown that there is a difference between ethylene and tetrafluoroethylene regarding the role that the resonances play in the elastic scattering cross section, in spite of the expectations that one might naively hold based on the similar symmetry of the two molecules. The present elastic scattering measurements show very little influence of the π^* resonance at 3 eV, unlike in the case of ethylene. This resonance does show up strongly in the complex Kohn calculation however, but this may be a consequence of the fact that this calculation was carried out at a single molecular geometry, and it may well get washed out if nuclear geometry effects are fully accounted for.[22] Furthermore, it is interesting to compare the role of the π^* resonance in the present measurements with that shown in the electron transmission (ETS) experiment of Chiu, Burrow, and Jordan.[2] This latter measurement is proportional to the derivative of the total cross section and the present EF results (admittedly only taken at selected scattering angles) lead one to conclude that elastic scattering must play a small part in the presence of this resonance in the ETS measurements.

There also remain several open questions regarding the exact interpretation of the 0.12 eV energy-loss peak which is seen in the energy-loss spectrum at 3 eV incident energy, and the origin of several resonance structures observed in both elastic and vibrational excitation functions. We hope that the present results, together with the new theoretical work, provide an improvement to the set of scattering cross sections for this molecule that are used in fluorocarbon discharge modeling.

ACKNOWLEDGMENTS

This work arose out of discussions with Skip Morgan and we gratefully acknowledge his input. It is a pleasure to acknowledge helpful communications with Professor Carl Winstead and Professor Paul Burrow, and we thank Professor Cz. Szmytkowski for providing us with tabulated results prior to publication. It is also a pleasure to acknowledge discussions with Cynthia Trevisan and Tom Rescigno who also sent tabulated data prior to publication. We are grateful to Michael Brunger for the phaseshift analysis leading to the integral cross section values. This project was supported in part by a grant from the Australian Research Council and the Japan Atomic Energy Research Institute.

[1] M. J. Coggiola, W. M. Flicker, O. A. Mosher, and A. Kuppermann, J. Chem. Phys. **65**, 2655 (1976).
[2] N. S. Chiu, P. D. Burrow, and K. Jordan, Chem. Phys. Lett. **68**, 121 (1979).
[3] Y. Jiang, J. Sun, and L. Wan, Phys. Rev. A **62**, 062712 (2000).
[4] C. Winstead and V. McKoy, J. Chem. Phys. **116**, 1380 (2002); C. Winstead (private communication).
[5] C. S. Trevisan, A. E. Orel, and T. N. Rescigno, Phys. Rev. A **70**, 012704 (2004).
[6] C. Szmytkowski, S. Kwitnewski, and E. Ptasinska-Denga, Phys. Rev. A (in press); (private communication).
[7] H. Jiang, D. Appadoo, E. Robertson, and D. McNaughton, J. Comput. Chem. **23**, 1220 (2002).
[8] J. R. Nielsen, H. H. Claassen, and D. C. Smith, J. Chem. Phys. **18**, 812 (1950).
[9] T. Shimanouchi, *Tables of Molecular Vibrational Frequencies* (National Bureau of Standards, Washington, DC, 1972), Vol. 1.
[10] G. Bélanger and C. Sandorfy, J. Chem. Phys. **55**, 2055 (1971).
[11] L. G. Christophorou and J. K. Olthoff, J. Phys. Chem. Ref. Data **30**, 449 (2001).
[12] K. Yoshida, S. Goto, H. Tagashira, C. Winstead, B. V. McKoy, and W. L. Morgan, J. Appl. Phys. **91**, 2637 (2002).
[13] R. Panajotovic, M. Kitajima, H. Tanaka, M. Jelisavcic, J. Lower, L. Campbell, M. J. Brunger, and S. J. Buckman, J. Phys. B **36**, 1615 (2003).
[14] M. Kitajima, Y. Sakamoto, R. J. Gulley, M. Hoshino, J. C. Gibson, H. Tanaka, and S. J. Buckman, J. Phys. B **33**, 1687 (2000).
[15] K. Rohr, J. Phys. B **10**, 2215 (1977).
[16] J. N. H. Brunt, G. C. King, and F. H. Read, J. Phys. B **10**, 1615 (1977).
[17] R. K. Nesbet, Phys. Rev. A **20**, 58 (1979).
[18] L. Boesten and H. Tanaka, At. Data Nucl. Data Tables **52**, 25 (1992).
[19] D. Fursa and I. Bray, J. Phys. B **30**, 757 (1997).
[20] H. Cho, R. J. Gulley, K. W. Trantham, L. J. Uhlmann, C. J. Dedman, and S. J. Buckman, J. Phys. B **33**, 3531 (2000).
[21] M. J. Brunger and S. J. Buckman, Phys. Rep. **357**, 215 (2002).
[22] T. N. Rescigno (private communication).